High-resolution microendoscopy: a point-of-care diagnostic for cervical dysplasia in low-resource settings

Benjamin D. Grant[a], José H.T.G. Fregnani[f], Júlio C. Possati Resende[g], Cristovam Scapulatempo-Neto[h,i], Graziela M. Matsushita[i], Edmundo C. Mauad[g], Timothy Quang[a], Mark H. Stoler[c], Philip E. Castle[d,e], Kathleen M. Schmeler[b] and Rebecca R. Richards-Kortum[a]

Cervical cancer is the third leading cause of cancer-related death among women in low-to-middle income countries. Pap testing and pathological services are difficult to implement under these settings. Alternative techniques for the diagnosis of cervical precancer in these settings are needed to reduce the burden of the disease. The objective of this study was to evaluate the diagnostic accuracy of a low-cost, high-resolution microendoscope imaging system in identifying precancerous lesions of the cervix *in vivo*. A retrospective study of 59 patients undergoing colposcopy for an abnormal Pap test was performed at Hospital de Câncer de Barretos in Brazil. All patients underwent colposcopy as per standard of care, and acetowhite lesions were recorded. High-resolution microendoscopy (HRME) images were obtained from one colposcopically normal region and from all lesions observed on colposcopy. Biopsies of abnormal areas were obtained and reviewed by three independent, blinded pathologists and compared with HRME findings. The mean nuclear area and the median nuclear eccentricity were calculated from HRME images acquired from each site. A diagnostic algorithm to distinguish histopathologically diagnosed cervical intraepithelial neoplasias of grade 2 or more severe lesions (high grade) from less severe lesions (low grade) was developed using these parameters. A test of trend was used to analyze the relationship between HRME positivity and severity of histopathogical diagnosis. Fisher's exact test was used to analyze differences in HRME positivity between high-grade and low-grade lesions. Evaluable images were obtained from 108 of 143 discrete sites. Of these, 71 sites were colposcopically normal or low grade according to histopathology and 37 were diagnosed as high grade on the basis of histopathology. Using the mean nuclear area and the median nuclear eccentricity, HRME images from 59 colposcopically abnormal sites were classified as high grade or low grade with 92% sensitivity and 77% specificity compared with histopathological findings. Increasing HRME positivity showed a significant trend with increasing severity of diagnosis ($P_{trend} < 0.001$). We found a strong association ($P < 0.001$) between HRME positivity and a histopathological diagnosis of cervical intraepithelial neoplasia of grade 2 or higher. HRME demonstrated an accurate in-situ diagnosis of high-grade dysplasia. In low-resource settings in which colposcopy and histopathology services are severely limited or unavailable, HRME may provide a low-cost, accurate method for diagnosis of cervical precancer without the need for biopsy, allowing for a single 'screen-and-treat' approach. ***European Journal of Cancer Prevention*** **26:63–70**

European Journal of Cancer Prevention 2017, **26**:63–70

Keywords: cervical cancer, cervical intraepithelial neoplasia, early detection of cancer

[a]Department of Bioengineering, Rice University, [b]Department of Gynecologic Oncology and Reproductive Medicine, The University of Texas, MD Anderson Cancer Center, Houston, Texas, [c]Department of Pathology, University of Virginia School of Medicine, Charlottesville , [d]Global Coalition against Cervical Cancer, Arlington, Virginia, [e]Department of Epidemiology and Population Health, Albert Einstein College of Medicine, Bronx, New York, USA, [f]Center for the Researcher Support, [g]Department of Cancer Prevention, [h]Molecular Oncology Research Center and [i]Department of Pathology, Pio XII Foundation, Barretos Cancer Hospital, Barretos, Brazil

Correspondence to Rebecca R. Richards-Kortum, PhD, 6500 Main Street, Houston, Texas 77030, USA
Tel: +1 713 348 5869; e-mail: rkortum@rice.edu

Received 9 July 2015 **Accepted** 5 November 2015

Introduction

There are more than 520 000 new cases of cervical cancer and 265 000 cervical cancer-related deaths annually (Torre *et al.*, 2015). More than 85% of cases of and deaths due to cervical cancer occur in low-income and middle-income countries, where cervical cancer is the third leading cause of cancer-related death among women (Torre *et al.*, 2015). Cervical cancer incidence and mortality rates are much lower in high-resource settings because of the implementation of organized screening programs based on Pap and/or HPV testing, diagnosis by colposcopy and biopsy, and timely treatment of cervical precancer and early-stage cancer. However, many low-income and middle-income countries have been unable to implement such screening programs because of the high cost of the necessary infrastructure and the lack of qualified personnel (Wright and Kuhn, 2012; López-Gómez *et al.*, 2013). Screening programs are also

DOI: 10.1097/CEJ.0000000000000219

hampered by loss to follow-up of screen-positive women, who do not receive accurate diagnosis and timely treatment. As a result, many women still die needlessly from cervical cancer.

The World Health Organization (WHO) recently recommended alternative screening strategies for HPV DNA or visual inspection with acetic acid (VIA) and screen-and-treat (S&T) protocols, in which traditional programs based on Pap testing and diagnosis have not been implemented (WHO, 2013). However, like Pap testing, both VIA and HPV testing have limited specificities – that is, the vast majority of screen-positive women do not have cervical precancer or cancer. HPV detection cannot distinguish between benign high-risk HPV infections destined to resolve and those associated with the development of preinvasive and invasive cancer. In a study of 31 343 women screened with VIA in India, VIA had a positive predictive value of only 9.2% for high-grade cervical precancer or cancer (Sankaranarayanan *et al.*, 2007). In a subsequent study, Sankaranarayanan *et al.* (2009) randomized 131 746 women in rural India to receive either a single lifetime screening test (i.e. cytology, VIA or HPV testing) or standard of care (cervical cancer health education). Both VIA and HPV testing were associated with low positive predictive values: 7.4% for VIA and 11.3% for HPV testing (Sankaranarayanan *et al.*, 2009). Therefore, using only HPV or VIA screening would lead to substantial overtreatment.

Thus, there is an important need for affordable tools to enable accurate, real-time diagnosis of cervical precancer and early invasive cancer in screen-positive women in low-resource settings. In an attempt to better detect early cervical neoplasia at the point of care in screen-positive women, flexible fiberoptic microscopes have been developed to provide real-time images of the morphologic features of the neoplasias *in vivo*. High-resolution optical techniques can image tissue with subcellular resolution to evaluate changes in epithelial morphology (Thekkek and Richards-Kortum, 2008). We developed a high-resolution microendoscope (HRME) capable of imaging epithelial cells *in vivo* (Muldoon *et al.*, 2007; Pierce *et al.*, 2011). The HRME utilizes a small (1 mm) fiberoptic probe placed in direct contact with the cervical epithelium, allowing real-time imaging of the underlying tissue. Utilizing the exogenous contrast agent proflavine, nuclear features including area, shape, and spacing can be observed in real time without the need for biopsy.

Pilot studies of this technology have demonstrated the potential to discriminate between neoplastic and non-neoplastic tissue in a variety of organ sites, including the esophagus (Pierce *et al.*, 2011; Thekkek *et al.*, 2012; Shin *et al.*, 2015), the oral cavity (Muldoon *et al.*, 2012; Pierce *et al.*, 2012b; Miles *et al.*, 2015), the colon (Parikh *et al.*, 2015), and the cervix (Pierce *et al.*, 2012a; Quinn *et al.*, 2012). In this pilot study in Barretos, Brazil, we evaluate the diagnostic accuracy of the HRME imaging system in identifying precancerous lesions of the cervix *in vivo*.

Methods

Study overview

The National Committee for Ethics in Research (CONEP) of Brazil and the Institutional Review Boards from Hospital de Câncer de Barretos (Barretos, Brazil), MD Anderson Cancer Center, and Rice University (Houston, Texas, USA) reviewed and approved this study. Female patients residing in the state of São Paulo, Brazil, were eligible to participate if they had been referred to Hospital de Câncer de Barretos for colposcopy because of a subset of abnormal Pap tests. Eligible referral Pap tests included low-grade squamous intraepithelial lesions, high-grade squamous intraepithelial lesions (HSILs), atypical squamous cells – cannot exclude HSIL (ASC-H), and atypical glandular cells. A Pap diagnosis of atypical squamous cells of undetermined significance was generally insufficient for inclusion, unless the patient had a previous, more severe Pap diagnosis. Exclusion criteria included women who were pregnant, had had a hysterectomy, or were nursing.

High-resolution microendoscope

The HRME is a battery-powered, fiberoptic fluorescence microscope. The design of the system has been described in detail previously (Muldoon *et al.*, 2007; Pierce *et al.*, 2011). The device is approved only for investigational use. An image of the system is provided in Fig. 1. The system is designed to image the cervical epithelium following topical application of proflavine, a fluorescent contrast agent that stains cell nuclei. Proflavine has a history of safe clinical use as a topical antiseptic (Wainwright, 2001), although its use as a contrast agent is investigational. Proflavine has a peak excitation wavelength of 445 nm and a peak emission wavelength of 510 nm. The HRME system provides excitation light to the tissue through a blue LED, with a center wavelength of 455 nm. The light is collimated, filtered, and directed into a 1.0-mm-diameter flexible fiberoptic bundle containing 30 000 individual fibers. The proflavine dye is applied topically to stain epithelial cell nuclei, and the fiber bundle is placed in gentle contact with the tissue site to be imaged. Proflavine fluorescence is then captured by the same fiberoptic bundle, filtered, and focused onto a battery-powered charge-coupled device sensor. The image is displayed in real-time on a laptop computer, which also controls image acquisition. The charge-coupled device captures video at 10 frames/s.

Study procedure

After consenting to participate in the study, each woman was first interviewed by a trained healthcare professional to obtain basic demographic information. All women underwent a urine-based pregnancy test before proceeding with the study. Next, routine colposcopy with

Fig. 1

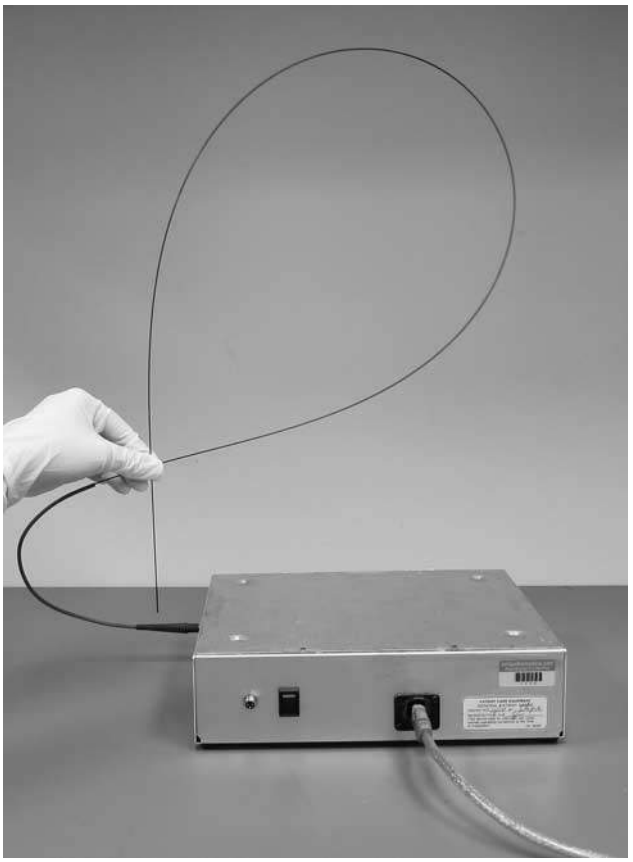

Picture of the high-resolution microendoscope (HRME) system (Quinn *et al.*, 2012).

5% acetic acid was performed to identify acetowhite lesions on the cervix. If acetowhite lesions were identified, 0.01% proflavine in sterile water was applied to the cervix using a spray bottle. The cervix was wiped with a cotton swab to ensure even distribution of proflavine. The clinician then applied 5% Lugol's iodine to the cervix, and any lesion that excluded iodine staining was noted. Finally, 0.01% proflavine was re-applied to ensure a strong fluorescence signal. The clinician then placed the distal tip of the fiber probe in gentle contact with each suspicious region identified during colposcopy and acquired a 2 s video from each site. The clinician also placed the HRME probe and acquired videos from a site that appeared by colposcopy to be normal squamous epithelium. The entire imaging procedure lasted less than 10 min. After HRME imaging was performed, a biopsy was obtained from each suspicious site and submitted for histopathological diagnosis.

Each biopsy was examined by two pathologists at Hospital de Câncer de Barretos, referred to in this manuscript as the clinical pathologists. All biopsies were also independently reviewed by a study pathologist at the University of Virginia. Samples were classified as normal, inflammation, cervical intraepithelial neoplasia (CIN) grade 1 (CIN1), CIN grade 2 (CIN2), CIN grade 3 (CIN3) or cancer on the basis of standard criteria (Richart, 1973). All pathologists were blinded to the HRME images and to the other pathologists' diagnoses. The two clinical pathologists came to a consensus diagnosis in any case in which their initial diagnoses disagreed. In cases in which the clinical pathologists' and study pathologists' diagnoses did not agree, the samples were classified as the more severely neoplastic diagnosis.

Data analysis

A researcher blinded to the histopathologic diagnosis selected the highest quality frame from each video with respect to clarity of focus. Sites were excluded from further analysis if more than 50% of the HRME image in the highest quality frame was out of focus or obscured by debris at the probe tip. The remaining images were analyzed using a custom Matlab 2012b script, designed to segment individual nuclei in each image and to quantify nuclear area and eccentricity. Briefly, the program first finds the outline of the fiber bundle and removes signal outside its boundary. Next, the image is Gaussian-filtered to remove image artifacts due to the outline of individual fiber cores in the image. After the Gaussian filter is applied, a top-hat filter is used to reduce background and increase contrast between nuclei and the background. This new image is used to automatically select a region of interest (ROI). The ROI is calculated automatically by first selecting the entire area inside the fiber boundary. Next, areas of the image that are too dimly lit, saturated, or homogeneous are removed from the ROI. After the final ROI is determined, a binary threshold is applied to segment individual nuclei from the background. The threshold value is chosen automatically by Otsu's method (Otsu, 1979). The nuclear-to-cytoplasmic ratio, the mean and median nuclear area, the SDs of the nuclear area, the median perimeter, and the median eccentricity are calculated and recorded for each image.

A test of trend (Cuzick, 1985) was used to examine the relationship between HRME categorizing the lesion as positive (CIN2+) and severity of histopathologic diagnosis by the study pathologists. Fisher's exact test was used to test for differences in HRME positivity for CIN2 or more severe diagnoses (CIN2+) versus <CIN2 diagnoses. Sensitivity, specificity, and odds ratios (ORs) with 95% confidence intervals (95% CIs) were calculated for HRME detection of CIN2+ and CIN3 or more severe diagnoses (CIN3+). *P*-values of less than 0.05 were considered statistically significant.

Results

A total of 59 patients were enrolled in the study between 17 June 2013 and 21 June 2013. All patients successfully underwent HRME imaging without any adverse event.

The median age was 34 years (range: 18–67 years). Referral Pap tests showed: atypical squamous cells of undetermined significance ($n=1$, 1.7%), low-grade squamous intraepithelial lesion ($n=7$, 11.9%), HSIL ($n=20$, 33.9%), ASC-H ($n=29$, 49.2%), and atypical glandular cells ($n=2$, 3.4%). HRME images were obtained from 84 colposcopically abnormal sites and 59 colposcopically normal sites. Fifty-nine of the 84 colposcopically abnormal sites imaged and biopsied were adequate for evaluation. Forty-nine of the 59 colposcopically normal sites imaged passed quality control review. Table 1 summarizes the colposcopic impression and consensus histologic diagnosis for the sites imaged with the HRME that passed quality control review.

Table 2 summarizes the agreement between the clinical and study pathologists for the sites with images passing quality control review. For 75% of these sites, the diagnoses provided by the clinical and study pathologists were identical. In cases in which the diagnosis differed, they did not disagree by more than one degree; for example, CIN2 versus CIN3.

Figure 2 shows representative HRME images for each histologic diagnosis, progressing from a normal squamous epithelium in Fig. 2a to CIN3 in Fig. 2f. The figure illustrates the changes seen in underlying nuclear size, shape, and crowding. Whereas normal tissue shows small, well-spaced uniform nuclei, high-grade dysplasia features large, crowded, irregularly shaped nuclei. In some cases, HRME images of CIN3 and cancer show prominent vessels (Fig. 2f). In this study, vessels were present in three of the 24 cases of CIN3 or cancer and were not present in any other histological classification.

We evaluated the ability of each quantitative nuclear feature to discriminate between <CIN2 and CIN2+. Two parameters – the mean nuclear area and the median nuclear eccentricity – provided the clearest delineation between neoplastic and non-neoplastic sites. Eccentricity is a measure of the circularity of an object; the higher the eccentricity the less circular the object is. As cells progress from low-grade to high-grade disease, their eccentricity and mean nuclear area both increase (Drezek *et al.*, 2003). Figure 3 shows a scatter plot graph of median nuclear eccentricity versus mean nuclear area for the 108 sites passing quality control. Using these two parameters, we were able to separate the 59 biopsied sites into <CIN2 and CIN2+ populations, with a sensitivity of 92% (34/37, 95% CI = 78.1–98.2%) and a specificity of 77% (17/22, 95% CI = 54.6–92.1%). The OR, as a measure of association and accuracy of HRME with CIN2+, was 38.5 (95% CI = 8.2–181). There was a significant trend of increasing HRME positivity with increasing severity of diagnosis ($P_{\text{trend}} < 0.001$), and HRME positivity was strongly associated with a CIN2+ diagnosis ($P < 0.001$). Using the same cutoff to separate biopsied sites into <CIN3 and CIN3+ results in a sensitivity of 96% (23/24, 95% CI = 78.8–99.3%) and a specificity of 54% (19/35, 95% CI = 36.7–71.2%). The OR for CIN3+ was 27.3 (95% CI = 3.3–225).

Figure 3 also shows the value of these parameters for the 49 colposcopically normal sites. All but three colposcopically normal sites were classified as non-neoplastic. Table 1 lists the fraction of sites that were classified as neoplastic according to these HRME parameters by colposcopic impression and histologic diagnosis, where available. All of the sites diagnosed as cancers and 95% of the sites diagnosed as CIN3 were correctly classified as neoplastic on the basis of HRME images. Only 6% of colposcopically normal sites were classified as HRME positive.

We also explored whether the fraction of sites classified as neoplastic was related to interobserver agreement between the clinical and study pathologists. Figure 4 shows a bar graph of the fraction of sites classified as neoplastic by the HRME versus the histologic diagnosis of the pathologists. In cases in which the clinical and study pathologists both provided a diagnosis of CIN1, only 29% of the samples were classified as neoplastic on the basis of the HRME image. In contrast, in cases in which the pathologists provided differing diagnoses of CIN1 or CIN2, 67% of the samples were classified as neoplastic by HRME imaging. Similarly, in cases in which the clinical and study pathologists both provided a diagnosis of CIN2, 90% of the samples were classified as neoplastic on the basis of the HRME image. In contrast, in cases in which the pathologists provided differing diagnoses of CIN2 or CIN3, 100% of the samples were classified as neoplastic by HRME imaging. Thus, if either the clinical or study pathologist classified the

Table 1 Fraction of sites classified as positive by HRME image analysis versus colposcopic impression and histologic diagnosis

Colposcopic impression	Histologic diagnosis	Number of sites measured passing QC review	Number of sites HRME positive	% HRME positive
Normal	NA	49	3	6
Abnormal	Normal/inflammation	8	2	25
Abnormal	CIN1	14	3	21
Abnormal	CIN2	13	11	85
Abnormal	CIN3	21	20	95
Abnormal	Cancer	3	3	100

The HRME system was used to collect images from 108 sites in 59 patients referred to Hospital de Câncer de Barretos between 17 June 2013 and 21 June 2013 on the basis of an abnormal Pap test. The colposcopic impression, histopathologic diagnosis, and HRME diagnosis are reported for each site passing quality control.
CIN, cervical intraepithelial neoplasia; HRME, high-resolution microendoscope; QC, quality control.

Table 2 Comparison of the histologic diagnosis made by the clinical pathologists and the study pathologist for all 59 colposcopically abnormal sites

	Study pathologist					
Clinical pathologists	Negative	CIN1	CIN2	CIN3	Cancer	Total
Negative	**8** **25% HRME +**	1 0% HRME+	0	0	0	9
CIN1	6 17% HRME+	**7** **29% HRME+**	3 67% HRME+	0	0	16
CIN2	0	0	**10** **90% HRME+**	2 100% HRME+	0	12
CIN3	0	0	2 100% HRME+	**17** **94% HRME+**	0	19
Cancer	0	0	0	1 100% HRME+	**2** **100% HRME+**	3
Total	14	8	15	20	2	59

The clinical pathologists were the two pathologists working at Hospital de Câncer de Barretos and the study pathologist refers to a blinded third pathologist at the University of Virginia. The bold text in the boxes along the diagonal indicates cases in which the clinical and study pathologists agreed exactly on the histologic diagnosis. In each category, the fraction of sites that was classified as neoplastic based on features of the HRME image is indicated.
CIN, cervical intraepithelial neoplasia; HRME, high-resolution microendoscope.

Fig. 2

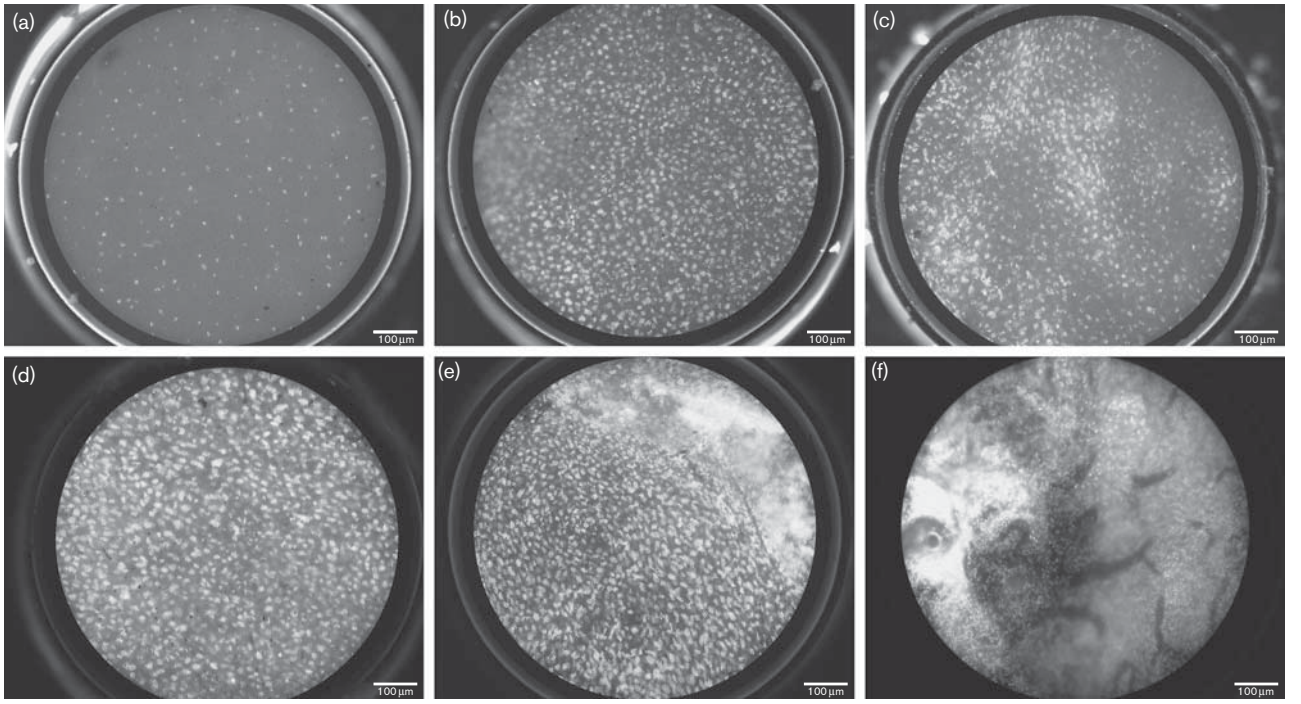

Representative HRME images of the cervical epithelium stained with proflavine and Lugol's iodine. (a) HRME image of a colposcopically normal site shows round, small, evenly spaced nuclei. (b–f) HRME images of colposcopically abnormal sites. (b) HRME image of a site with a histologic diagnosis of inflammation, characterized by evenly spaced, small, crowded nuclei. (c) HRME image of a site with a histologic diagnosis of CIN1, with slightly enlarged, evenly spaced nuclei. (d) HRME image of a site with a histologic diagnosis of CIN2 with enlarged, crowded, pleomorphic nuclei. (e) HRME image with a histologic diagnosis of CIN3 showing similar features to CIN2, with more pronounced nuclear crowding and pleomorphism. (f) HRME image of a second site diagnosed as CIN3 with very prominent vessels visible. CIN, cervical intraepithelial neoplasia; HRME, high-resolution microendoscope.

biopsy as high grade, the HRME diagnosis was more likely to be positive.

Discussion

This pilot study demonstrates the ability to use parameters derived from HRME images to objectively discriminate between non-neoplastic and neoplastic cervical tissue with a low false-negative and false-positive rate. Two of the three sites that were falsely classified as negative on the basis of HRME image parameters had a histologic diagnosis of CIN2, a less reproducible and reliable diagnosis than CIN3 (Carreon *et al.*, 2007). One additional possible cause for the false negatives in this study is imperfect correlation between the imaged

Fig. 3

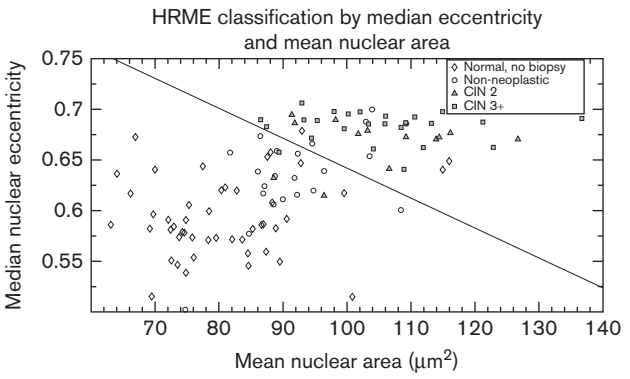

Scatter plot of the mean nuclear area versus the median nuclear eccentricity calculated from HRME images for each site. The gold standard histologic diagnosis for colposcopically abnormal sites that were biopsied is indicated by the marker shown in the legend. The gold standard histologic diagnosis is defined as the more severe diagnosis between the clinical pathologists' consensus diagnosis and the study pathologist's diagnosis. The black line was selected to maximize accuracy for separation of neoplastic (CIN2+) and non-neoplastic (<CIN2 – i.e. normal, inflammation, CIN1) sites. CIN, cervical intraepithelial neoplasia; HRME, high-resolution microendoscope.

Fig. 4

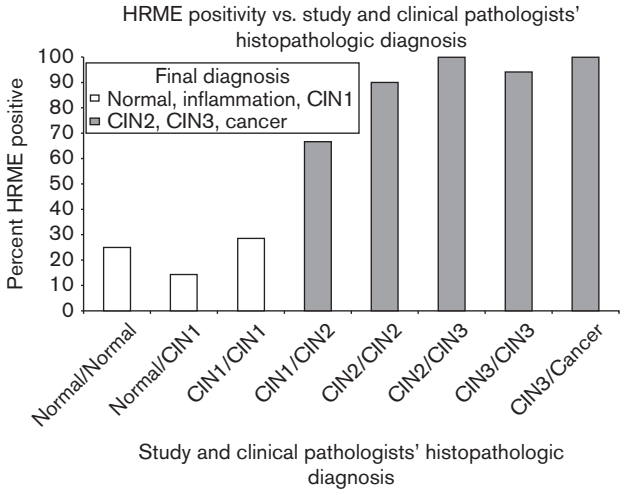

Bar graph depicting the percentage of sites classified as neoplastic on the basis of features of the HRME image versus clinical and study pathologists' histologic diagnosis. CIN, cervical intraepithelial neoplasia; HRME, high-resolution microendoscope.

location and the biopsy location. In the future, mosaicking could be implemented to acquire HRME images from a larger field of view in the ROI, reducing the chance of missing focal lesions (Bedard *et al.*, 2012). All four of the sites (100%) classified as CIN2 by one pathologist and CIN3 by another pathologist were classified as neoplastic according to the HRME algorithm. However, when the clinical and study pathologists agreed on a CIN2 diagnosis, the HRME-based algorithm was falsely negative for one of 10 sites (10%); when they disagreed between a diagnosis of CIN1 and CIN2, one of three (33%) samples was falsely classified as negative. These results suggest that the HRME-based algorithm may identify nuclear changes present in more advanced CIN2 cases; however, a larger study is necessary to validate this finding.

The sensitivity and specificity reported here are for the 59 sites that were colposcopically abnormal – that is, the subset of sites exhibiting acetowhitening. In a VIA screen-and-treat program, all 59 of these sites would be treated, including the 22 sites that were histologically non-neoplastic. Only five of these 22 (23%) sites were falsely classified as positive by HRME image analysis. Thus, in this study, the HRME would reduce overtreatment compared with that when using VIA by 77%. It is not possible to determine if the images from colposcopically normal locations that were classified as abnormal by HRME are truly falsely positive because these sites were not biopsied. These results support the concept that HRME image parameters could be used to improve the specificity of screen-and-treat programs by quantitatively identifying nuclear features associated with neoplasia, without requiring a biopsy and pathology services.

The 92% sensitivity and 77% specificity of the algorithm based on HRME image parameters reported here compare favorably with a previous study that our group performed in China (sensitivity = 100% and specificity = 67%; Pierce *et al.*, 2012a). In the previous study, the authors used the nuclear-to-cytoplasmic ratio to discriminate between neoplastic and non-neoplastic sites. The majority of the false-positive sites (17/19, 89%) in the China study were sites with underlying chronic inflammation. One concern was that in low-resource settings, the higher rates of inflammation would lead to lower HRME-based specificity. Indeed, using only the nuclear-to-cytoplasmic ratio to classify the images acquired in the current study resulted in a sensitivity of 76% and a specificity of 45%. We found that utilizing the mean nuclear area and the median eccentricity helped reduce the number of false positives. We hypothesize that these parameters are less susceptible to change due to inflammation than the nuclear-to-cytoplasmic ratio, as inflammation can lead to an increase in the nuclear-to-cytoplasmic ratio due to nuclear crowding. Conversely, nuclear area remains small and nuclei do not exhibit significant pleomorphism. The addition and utilization of these parameters helped improve both sensitivity and specificity in this study population; however, more data are needed to validate inclusion of this parameter in HRME image classification.

Although the results of this study are encouraging, there are limitations. Only 59 women were included in this

pilot study. A larger prospective study is necessary to validate the algorithm. In addition, lesions that are not visible by VIA will be missed by this modality. Furthermore, the HRME images from 30% of the sites that were biopsied did not pass quality control. This would result in an unacceptably high proportion of patients not receiving a diagnosis by HRME. To eliminate this problem, the software in future iterations of the device will provide feedback to the user to indicate whether an in-focus image was acquired. If the image is out of focus, the user will be prompted to acquire another image until an image of sufficient quality is obtained. After an image of sufficient quality is obtained, it will be analyzed immediately to provide an objective classification of the underlying tissue as low-grade or high-grade. The end user will not be required to interpret the mean nuclear area and median eccentricity but will instead receive a direct diagnosis of 'high grade' or 'not high grade' from the software. This automated software has been developed and will be validated in a future study. The HRME system costs approximately $5000 and the cost of the reagents is negligible. We are currently testing versions of the device that cost under $2000 to better facilitate their use in low-resource settings.

Further evaluation of the HRME modality in a large prospective study is ongoing. Our results suggest that HRME imaging may provide a low-cost, accurate, point-of-care alternative to colposcopy and directed cervical biopsies for the diagnosis of cervical dysplasia in lower-resource settings in which there is often a lack of colposcopy and pathology services. Some settings may not accept a screen-and-treat strategy because of concerns of overtreatment and yet lack the diagnostic capacity to provide a biopsy-proven diagnosis. In these settings, we envision the technology being used in conjunction with VIA or HPV DNA screening. Women who screen positive would then be evaluated with the HRME for immediate treatment if indicated, thereby reducing losses to follow-up.

Acknowledgements

This project has been funded in whole or in part with Federal funds from the National Cancer Institute, National Institutes of Health, under Contract No. HHSN261200800001E.

This material is based on work supported by the National Science Foundation Graduate Research Fellowship Program under Grant No. 0940902.

The authors thank Talita Garcia do Nascimento and Ligia Zampieri de Brito from Hospital de Câncer de Barretos, as well as Cindy Melendez and Juana Rayo from MD Anderson Cancer Center, for helping in research logistics.

Conflicts of interest

Dr Castle has received commercial HPV tests for research at a reduced cost or at no cost from Roche, Qiagen, Norchip, MTM, BD, and Arbor Vita Corporation. Dr Castle has been compensated financially as a member of a Merck Data and Safety Monitoring Board for HPV vaccines. Dr Castle has been paid as a consultant for BD, Gen-Probe/Hologic, Roche, Cepheid, ClearPath, Guided Therapeutics, Teva Pharmaceuticals, Inovio Pharmaceuticals, Genticel and GE Healthcare. Dr Castle has received honoraria as a speaker for Roche and Cepheid. Dr Richards-Kortum serves as an unpaid scientific advisor to Remicalm LLC, holds patents related to optical diagnostic technologies that have been licensed to Remicalm LLC, and holds minority ownership in Remicalm LLC.

References

Bedard N, Quang T, Schmeler K, Richards-Kortum R, Tkaczyk TS (2012). Real-time video mosaicing with a high-resolution microendoscope. *Biomed Opt Express* **3**:2428–2435.

Carreon JD, Sherman ME, Guillén D, Solomon D, Herrero R, Jerónimo J, *et al.* (2007). CIN2 is a much less reproducible and less valid diagnosis than CIN3: results from a histological review of population-based cervical samples. *Int J Gynecol Pathol* **26**:441–446.

Cuzick J (1985). A Wilcoxon-type test for trend. *Stat Med* **4**:543–547.

Drezek R, Guillaud M, Collier T, Boiko I, Malpica A, Macaulay C, *et al.* (2003). Light scattering from cervical cells throughout neoplastic progression: influence of nuclear morphology, DNA content, and chromatin texture. *J Biomed Opt* **8**:7–16.

López-Gómez M, Malmierca E, de Górgolas M, Casado E (2013). Cancer in developing countries: the next most preventable pandemic. The global problem of cancer. *Crit Rev Oncol Hematol* **88**:117–122.

Miles BA, Patsias A, Quang T, Polydorides AD, Richards-Kortum R, Sikora AG (2015). Operative margin control with high-resolution optical microendoscopy for head and neck squamous cell carcinoma. *Laryngoscope* **125**: 2308–2316.

Muldoon TJ, Pierce MC, Nida DL, Williams MD, Gillenwater A, Richards-Kortum R (2007). Subcellular-resolution molecular imaging within living tissue by fiber microendoscopy. *Opt Express* **15**:16413–16423.

Muldoon TJ, Roblyer D, Williams MD, Stepanek VM, Richards-Kortum R, Gillenwater AM (2012). Noninvasive imaging of oral neoplasia with a high-resolution fiber-optic microendoscope. *Head Neck* **34**:305–312.

Otsu N (1979). A threshold selection method from gray-level histograms. *IEEE Trans Syst Man Cybern* **9**:62–66.

Parikh ND, Perl D, Lee MH, Chang SS, Polydorides AD, Moshier E, *et al.* (2015). In vivo classification of colorectal neoplasia using high-resolution microendoscopy: improvement with experience. *J Gastroenterol Hepatol* **30**:1155–1160.

Pierce M, Yu D, Richards-Kortum R (2011a). High-resolution fiber-optic microendoscopy for in situ cellular imaging. *J Vis Exp* **47**:pii: 2306. doi: 10.3791/2306.

Pierce MC, Vila PM, Polydorides AD, Richards-Kortum R, Anandasabapathy S (2011b). Low-cost endomicroscopy in the esophagus and colon. *Am J Gastroenterol* **106**:1722–1724.

Pierce MC, Guan Y, Quinn MK, Zhang X, Zhang WH, Qiao YL, *et al.* (2012a). A pilot study of low-cost, high-resolution microendoscopy as a tool for identifying women with cervical precancer. *Cancer Prev Res (Phila)* **5**:1273–1279.

Pierce MC, Schwarz RA, Bhattar VS, Mondrik S, Williams MD, Lee JJ, *et al.* (2012b). Accuracy of in vivo multimodal optical imaging for detection of oral neoplasia. *Cancer Prev Res (Phila)* **5**:801–809.

Quinn MK, Bubi TC, Pierce MC, Kayembe MK, Ramogola-Masire D, Richards-Kortum R (2012). High-resolution microendoscopy for the detection of cervical neoplasia in low-resource settings. *PLoS One* **7**:e44924.

Richart RM (1973). Cervical intraepithelial neoplasia. *Pathol Annu* **8**:301–328.

Sankaranarayanan R, Esmy PO, Rajkumar R, Muwonge R, Swaminathan R, Shanthakumari S, *et al.* (2007). Effect of visual screening on cervical cancer incidence and mortality in Tamil Nadu, India: a cluster-randomised trial. *Lancet* **370**:398–406.

Sankaranarayanan R, Nene BM, Shastri SS, Jayant K, Muwonge R, Budukh AM, *et al.* (2009). HPV screening for cervical cancer in rural India. *N Engl J Med* **360**:1385–1394.

Shin D, Protano MA, Polydorides AD, Dawsey SM, Pierce MC, Kim MK, *et al.* (2015). Quantitative analysis of high-resolution microendoscopic images for diagnosis of esophageal squamous cell carcinoma. *Clin Gastroenterol Hepatol* **13**:272–279.e2.

Thekkek N, Richards-Kortum R (2008). Optical imaging for cervical cancer detection: solutions for a continuing global problem. *Nat Rev Cancer* **8**:725–731.

Thekkek N, Muldoon T, Polydorides AD, Maru DM, Harpaz N, Harris MT, *et al.* (2012). Vital-dye enhanced fluorescence imaging of GI mucosa: metaplasia, neoplasia, inflammation. *Gastrointest Endosc* **75**:877–887.

Torre LA, Bray F, Siegel RL, Ferlay J, Lortet-Tieulent J, Jemal A (2015). Global cancer statistics, 2012. *CA Cancer J Clin* **65**:87–108.

Wainwright M (2001). Acridine – a neglected antibacterial chromophore. *J Antimicrob Chemother* **47**:1–13.

WHO (2013). *Guidelines for screening and treatment of precancerous leasions for cervical cancer protection*. Geneva: WHO.

Wright TC Jr, Kuhn L (2012). Alternative approaches to cervical cancer screening for developing countries. *Best Pract Res Clin Obstet Gynaecol* **26**: 197–208.